Biomimetic design of elastomer surface pattern for friction control under wet conditions

2013 Bioinspir. Biomim. 8 046001

(http://iopscience.iop.org/1748-3190/8/4/046001)

Bioinspir. Biomim. **8** (2013) 046001 (6pp) doi:10.1088/1748-3182/8/4/046001

Biomimetic design of elastomer surface pattern for friction control under wet conditions

Wei Huang[1,2] **and Xiaolei Wang**[1,2,3]

[1] College of Mechanical and Electrical Engineering, Nanjing University of Aeronautics and Astronautics, Nanjing 210016, People's Republic of China
[2] Jiangsu Key Laboratory of Precision and Micro-Manufacturing Technology, Nanjing 210016, People's Republic of China

E-mail: wxl@nuaa.edu.cn

Received 17 June 2013
Accepted for publication 7 August 2013
Published 3 September 2013
Online at stacks.iop.org/BB/8/046001

Abstract

In this paper, an observation on the toe pad of a newt was carried out. It was found that the pad surface is covered with an array of polygonal cells separated by channels, similar to those of a tree frog's pad. With this micro-structure, a newt can move on wet and smooth surfaces without slipping. Inspired by the surface structure of newt toe pads, elastic micro-patterned surfaces were fabricated to understand the function of such micro-structures in friction systems. The tribological performance of the patterned surfaces was evaluated using a tribometer. Different tribological performances between micro-dimple and -pillar patterned surfaces were observed. The area density (r) of the micro-pattern is crucial for controlling the friction of the elastic surface. Distinguished from unpatterned and micro-dimple patterned surfaces, the pillar patterned surface with high area density can remain high friction at high sliding speed. It could be one of the reasons of such polygonal structures on newt's toe pads.

(Some figures may appear in colour only in the online journal)

1. Introduction

In the process of biological evolution, nature has created many incredible surfaces in animals and plants. For example, the leaves of the lotus flower exhibit high water repellence, which results from tiny wax-coated protuberances on their surface [1]. Waterstriders have the ability to stand and walk on a water surface without becoming wet because of the numerous oriented setae on their legs [2]. Geckos have compliant high aspect ratio beta-keratin structures on their feet to adhere to most surfaces [3]. Scientists have gradually understood that each of these remarkable phenomena originates from the presence of micro- and nano-scale textures on the surfaces covering the bodies of animals and plants [4]. Nowadays, surface texturing has been proved to be an effective technique to improve tribological performance of machine components [5].

Here, we study an ancient amphibian, the newt, which evolved during the middle Jurassic period. The whole size of the newt used in this study was about 6–7 cm, as noted in figure 1(a). It can move on wet and almost vertical glass surface without slipping, similar to a gecko climbing a wall. This ability may be closely related to the micro-structure of newts' toe pads. We observed its toe pads by using scanning electron microscopy (SEM) and found that the pad shows characteristic polygonal cells of approximately 30 μm in size (see figure 1(b)) separated by narrow networking grooves of about 0.5 μm (see figure 1(c)). Each of the cells contains countless hemispheric bulges of approximately 300 nm surrounded by smaller channels (see figure 1(d)).

Interestingly, the surface micro-structure is similar to that of tree frogs' toe pads, which have largely hexagonal columnar epithelial cells separated by mucous-filled channels [6–8]. The

[3] Author to whom any correspondence should be addressed.

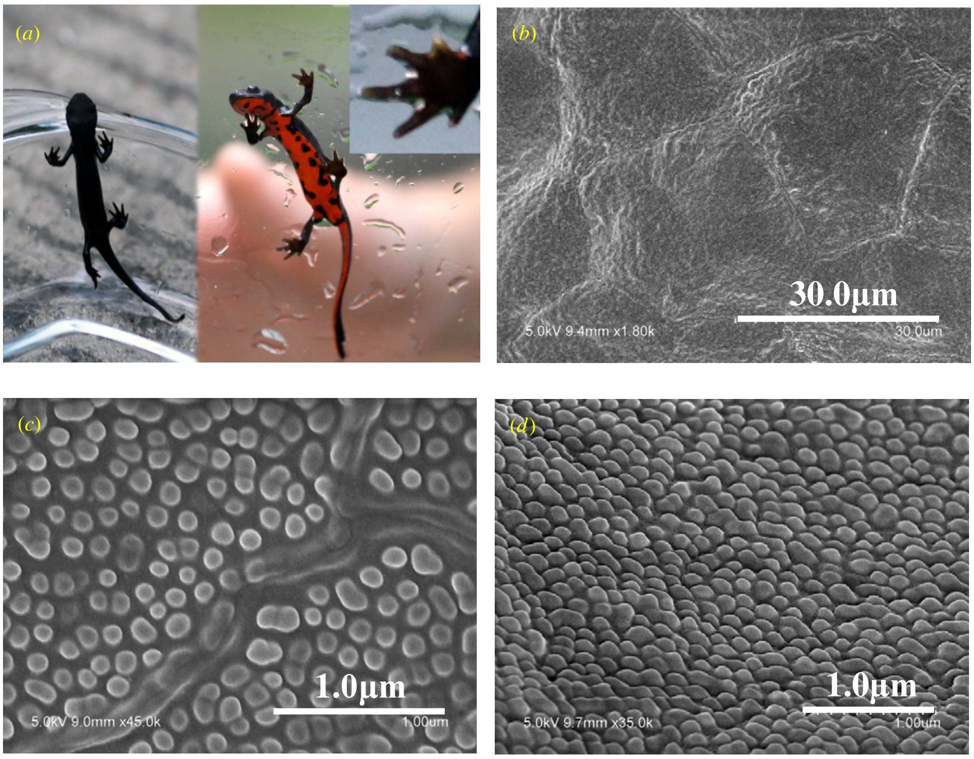

Figure 1. (*a*) Image of a newt creeping on wet glass; (*b*) scanning electron microscopy (SEM) of toe pad epithelium showing the polygonal cell structure separated by grooves; (*c*) magnified image of the networking grooves; (*d*) magnified region of a single polygonal cell depicting hemispheric bulges.

toe pads of tree frogs became a research hotspot because of the frogs' ability to climb in humid environments without falling. Hexagonal convex structures were also found in the foot pads of katydids and bush crickets [9, 10]. In recent decades, much attention has been paid to the adhesion properties of these micro-patterned toe pads. It was believed that the special adhesion function is mainly due to the hexagonal pillared structure and the liquid stored in the channels, which can form capillary bridges to generate adhesive forces [9, 11]. To date, the adhesive mechanisms of the channel structure have been extensively studied both theoretically and experimentally [6, 7, 11–13]. In view of the importance of locomotion, however, friction forces have received much less attention than adhesive forces until recently [14]. Persson noted that the hexagonal pillar structure allows frogs to expel fluid from the contact area and to achieve high friction forces [11]. The frictional properties of the hexagonal pillar structure in wet conditions were studied by Drotlef *et al*, and the micro-structure surfaces show significantly higher frictions than flat surfaces in the presence of a wetting liquid at speed of 100 μm s^{-1} [8].

From a tribological point of view, some uncertainties still exist. As raised by Varenberg and Grob [15], why was the polygonal pillar structure, rather than the round structure, evolved during the biological evolutionary process? Compared with a micro-dimple patterned surface, is there any advantage to the channel structure (pillar patterned surface) for tree frogs or newts in wet conditions? What is the relationship between the frictional properties and the area density of the micro-pattern on rubbing surfaces? With the development of micro-fabrication techniques, it is convenient to prepare a surface with well-controlled micro-patterns having specific geometrical characteristics. Such surfaces provide unique tools to experimentally answer the above questions.

In this paper, inspired by the structure observed on a newt's toe pads, patterned surfaces with/without channelled structures were fabricated, and the effects on the friction of elastomer contact were studied. The geometrical shapes of the micro-pattern, as well as the pattern area density, were taken into account. A soft elastomeric material, polydimethylsiloxane (PDMS), was used for test specimen fabrication because of its low surface energy and weak chemical reactivity [16]. Patterns of micro-dimples and -pillars were fabricated on the surfaces of PDMS disks. The tribological performance of spherical PDMS pins sliding on patterned versus flat disks was investigated.

2. Experimental section

2.1. Specimen fabrication

The tribopairs (spherical pins and disks) were both made of the same commercially available elastomer, Polydimethylsiloxane prepolymer Sylgard 184, purchased from Dow Corning (MI, USA). Micro-dimple/pillar arrayed structures with different parameters were fabricated on the disk surfaces by the lithography and replica technique, as mentioned in [17, 18]. The diameter of the PDMS disk was 36 mm, and the thickness was 5 mm. Three types of patterns were designed on the disk surface: round dimple, round pillar and hexagonal pillar. Figure 2(*a*) shows the configuration of the round and hexagonal

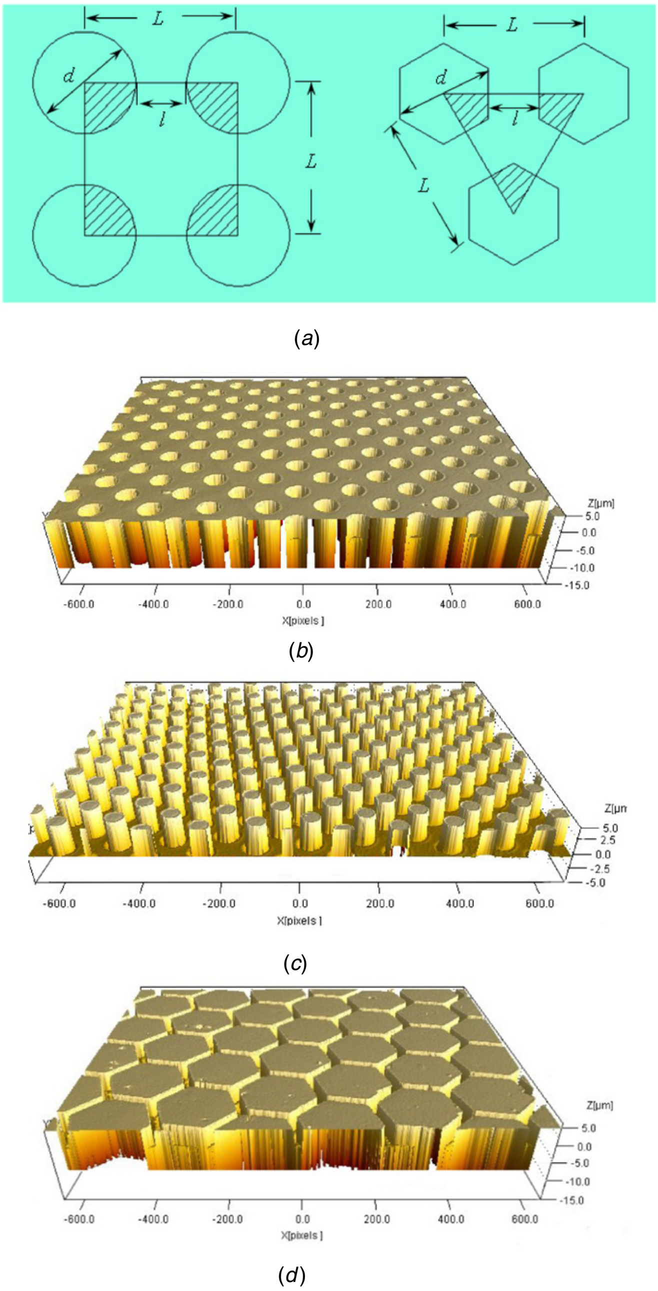

Figure 2. Configuration mode and 3D profile of several patterns used in this study: (*a*) configuration mode of the round and hexagonal patterns; (*b*) round dimple pattern with $r = 22.9\%$; (*c*) round pillar pattern with $r = 29.9\%$; (*d*) hexagonal pillar pattern with $r = 79.7\%$.

micro-structures. The area density (r) can be defined as the ratio of the area of round (or hexagon) structures over the whole sample area. The area density and the edge space of the round and hexagon patterns were calculated as follows:

$$r_R = \frac{\pi d^2}{4L^2} \quad (1)$$

$$l_R = L - d \quad (2)$$

$$r_H = \frac{3d^2}{4L^2} \quad (3)$$

$$l_H = L - \frac{\sqrt{3}}{2}d, \quad (4)$$

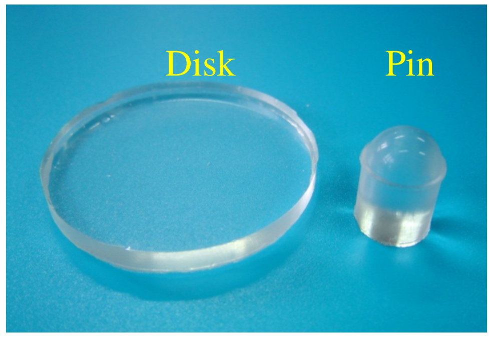

Figure 3. Image of the tribopair.

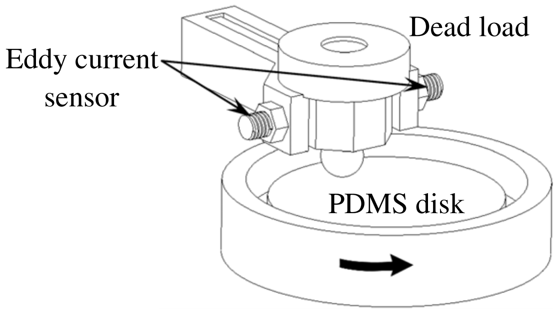

Figure 4. Scheme of the experimental apparatus.

where L is the pitch, d is the diameter/the diameter of the hexagon's circumscribed circle, r_R and r_H are the area densities of round and hexagonal patterns, respectively, and l_R and l_H are the edge spaces of the two patterns. Note that the area density (r) and edge space (l) for the round dimples and pillars are calculated using the same equations (equations (1) and (2)). The pattern parameters are listed in table 1. The 3D images of several patterned samples used in this study are presented in figures 2(*b*)–(*d*).

Figure 3 shows an image of the tribopair (PDMS disk and pin). The roughness of the PDMS disk was measured by surface mapping microscope (Rtec instruments, USA), and the results indicated that the PDMS disks had an average surface roughness Ra of approximately 140 nm. The surface wettability of the PDMS was evaluated by the water contact angle on its surface. Tests indicated that the surface of PDMS was hydrophobic, with a water contact angle of 112 ± 2 degrees.

Using a spherical mould, a spherical pin made of PDMS was prepared. The spherical radius of the pins was 6.35 mm, with a surface roughness of approximately 20–30 nm.

2.2. Friction test

The friction tests were performed on a pin-on-disk tribometer as shown in figure 4. The spherical pin was stationary and held by a bending beam. A normal load was applied to the pin with a dead weight. The disk was driven by a motor rotating at a constant speed. An eddy current sensor was fixed at the end of the beam, and the friction force was obtained by measuring the strain of the beam caused by friction. The output voltage

Table 1. Parameters of the dimple and pillar patterns.

	Parameters				
Patterns	Diameter d (μm)	Pitch L (μm)	Space l (μm)	Depth/height h (μm)	Area ratio r (%)
Round dimple	50	275–70	225–20	5	2.6–40.1
Round pillar	50	275–70	225–20	5	2.6–40.1
Hexagonal pillar	200	273–194	100–20	5	40.2–79.7

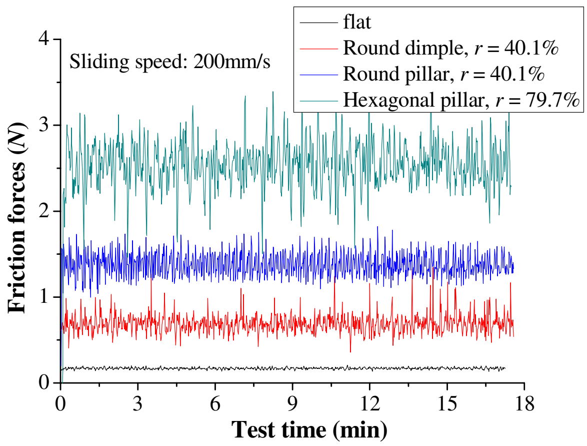

Figure 5. Variation of friction curves for different specimens.

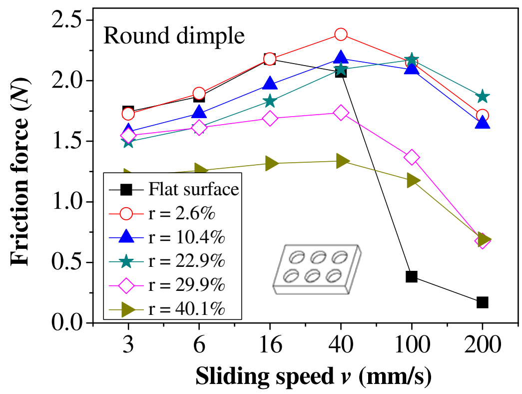

Figure 6. Evolution of friction behaviour of flat and round dimple pattern surfaces with sliding speed.

signals from the sensor were sampled with a data acquisition board PCI6221. All data were processed with the LabVIEW software package.

For each test, the pin was brought into contact with the sample disk lubricated with deionized water. The normal load was controlled at 0.95 N, and the sample was moved at speeds (v) of 3–200 mm s^{-1} for 15 min. The main aim of the experiments was to figure out the effect of different surface patterns on the friction properties, though the experimental parameters may not be appropriate for the natural system. The variations of the friction curves for several specimens are shown in figure 5, and the obvious curve fluctuation for the patterned surface may be due to tribopair contact discontinuity. The friction forces during the last 5 min were averaged and used as an index for evaluating the effects of the surface. To ensure the accuracy and reliability of the experimental data, each test was repeated three times, and the final force was the mean value of the three trials. In addition, because the mechanical properties of PDMS may change over time, all friction experiments were performed on one-day-old samples.

3. Results and discussion

Figure 6 shows the variation of friction forces with sliding speed for the flat and micro-dimple patterned surfaces. Significant differences were observed in the friction behaviours between the two types of disks, especially at high speeds. With a flat disk, the friction trend showed a clear transition from a high friction force of approximately 1.74 N at the minimum speed (3 mm s^{-1}) to the much lower value of 0.16 N at the maximum speed (200 mm s^{-1}). This trend suggests that the friction behaviour moved from the boundary to the mixed lubrication regime according to the corresponding friction coefficient of 1.83 and 0.17. Similar high friction performances of disks with lower pattern densities were found at low sliding speeds (v <40 mm s^{-1}). However, with an increase in the dimple area density, an obvious reduction in friction appeared at a low sliding speed (v <40 mm s^{-1}), and the sample with a density of 40.1% displayed the lowest friction force. The friction forces decreased from approximately 2.38 N (pattern with r = 2.6%) to 1.33 N (pattern with r = 40.1%) at a sliding speed of 40 mm s^{-1}, which represents a significant decrease of 44%.

Because of the hydrophobic property of the PDMS, the lubricant was easily displaced from the contact area at low sliding speeds, forming dry friction. As observed by Martin *et al* [19], the dry contact of rubber squeezing a non-wetting liquid against a plate at a low sliding speed and boundary friction may be based on the formation of dry contacts. Moreover, affected by the work of adhesion, the friction force of the elastomer increases in proportion to the real contact area [20]. The existence of the dimple patterns undoubtedly decreased the dry contact area, thereby partially decreasing the friction.

At higher sliding speeds, the differences in the friction between the two types of disks became significant because of the influence of the lubricant film. For the flat surface, a continuous fluid film formed, as indicated by the lower friction forces. The direct contact of the friction plates was prevented by the water film, corresponding to hydroplaning [19]. However, the ability to retain liquid in the dimple pattern helps to form hydrodynamic effect [21], which would be useful for reducing the friction. Unlike the channelled grooves, the micro-dimple is an enclosed structure that acts as a liquid reservoir. The lubricant stored in the dimples could be squeezed out to form local lubrication [17]. The effect of squeezing lubrication tends to be high as the dimple area

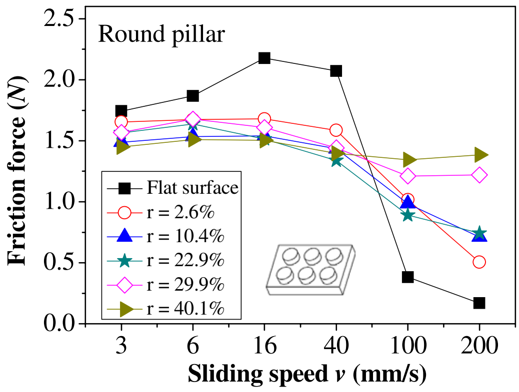

Figure 7. Evolution of friction behaviour of flat and round pillar pattern surfaces with sliding speed.

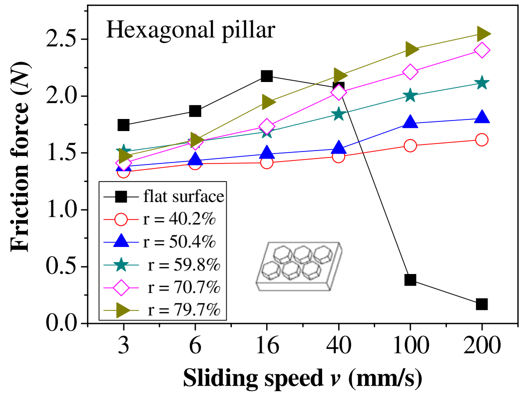

Figure 8. Evolution of friction behaviour of flat and hexagonal pillar pattern surface with sliding speed.

density increases; thus, disks with higher dimple densities could achieve lower friction at higher sliding speeds.

Figure 7 presents the friction force as a function of sliding speed for the flat and round pillar channelled surfaces. Similar to the dimple-patterned surface, the specimens with round pillars also showed friction reduction to a certain degree at a low sliding speed (v <40 mm s^{-1}), which may have been caused by a reduction in contact area. However, compared to the flat surface, the friction forces of the specimens with a pattern area density of 40.1% were stable and presented a significantly large force of approximately 1.38 N at a sliding speed of 200 mm s^{-1}. A similar phenomenon appears for specimen with pattern density of 29.9%.

In general, the friction forces of all the disks with round pillar patterns decreased with an increase in sliding speed. Disks with lower area densities clearly remained in the mixed lubrication regime at the maximum speed of 200 mm s^{-1}, while the higher density samples may have remained in the boundary regime, as implied by the calculated friction coefficients. Interestingly, unlike the micro-dimple surface, the pillar patterned specimens with high area density still remained high friction at high sliding speed and the forces increased with the increase of pillar densities. One possible reason for this finding is the networking structure of the pillar patterns, which can drain water off the contact surface through the channels. At the same time, once the upper pin slid against the patterned disk, the micro-pillar bent and bore tangential and normal loads on its edge. Thus, the increase of pattern density, which promotes the edge contact frequency, could be another reason for the finding.

An interesting question arose: what would the friction properties be with a further increase in pillar pattern area density? By geometric analysis, it is known that the area density (r) of the patterns is related to the geometrical shape of a single micro-structure. Inspired by the micro-structure of newt's toe pads, a hexagonal structure was introduced (see figure 2).

Given the minimum edge space $l_R = 20\ \mu$m (see table 1), the maximum area density of the round pattern with a diameter of 50 μm can only reach 40.1%, according to equation (1). While the minimum edge space (l_H) remains 20 μm, the maximum area density (r_H) of the hexagonal micro-pattern can be as high as 79.7% if the diameter increases to 200 μm. Thus, the effects of higher density pillar patterns on friction properties can be studied by means of hexagonal micro-patterned surfaces. Although the size of the micro-structure is much larger than the features of newt's toe pads, the design idea originates from bionic principle.

Figure 8 represents the evolution of the friction forces of flat and hexagonal pillar patterned surfaces with the different sliding speeds. As observed, the flat disk displayed higher friction than the micro-structured disks at low speeds (v <40 mm s^{-1}). In the high-speed region (v > 40 mm s^{-1}), all of the friction forces were well above those of the flat disks. Surprisingly, the forces of all patterned samples increased smoothly with increasing sliding speed and the friction forces did not show any transition with sliding speed, which is different from flat and dimple patterned surfaces. It indicated that such high densities of micro-structures are conducive to achieving stable friction from low to high sliding speed. Similar velocity-dependence of the shear force of a single tree frog toe pad was reported in [13].

As shown in figure 8, the pillar area density greatly affected the tribological performance of the patterned surfaces and the friction force increases with the increasing area density. Possible reasons for this finding are as follows. (1) As mentioned above, the network of the channels on the surface facilitates the expulsion of the fluid between contact surfaces. Due to the higher pillar densities, the lubricant favours draining of the contact surface from the narrower channels because of capillary suction [6], which more easily forms dry friction. (2) During the friction experiment, an energy barrier must be overcome when the upper pin slides over the channel edges. Obviously, the channel edge is also related to pattern density. Therefore, the hexagonal pillar pattern surfaces show obvious friction increases with the increase of area density.

The impacts of the pillar (round and hexagonal) area density on friction forces at low and high sliding speeds are summarized in figure 9. The solid marks represent low sliding speed of 3 mm s^{-1} and the open marks represent 200 mm s^{-1}. As can be seen in figure 9 the area density appeared to have little effect on friction at a low sliding speed, and the forces remained nearly constant. At a high speed of 200 mm s^{-1}, clear friction enhancement was observed with increasing pillar density. This finding indicates that pillar patterns helped to achieve higher friction, but only at higher sliding speeds. The

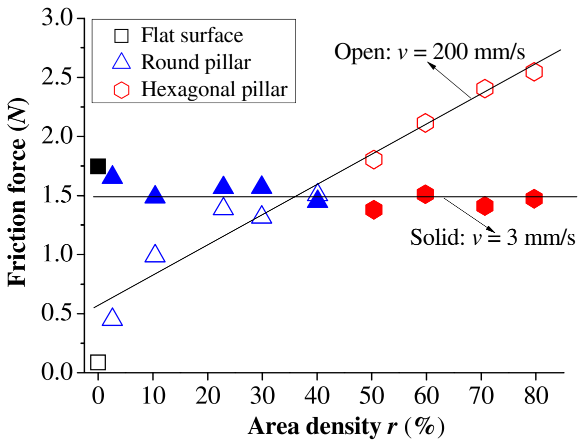

Figure 9. Summary of friction forces with area density for pillar patterns at low and high speeds.

greater the pattern density of the surface, the higher the friction it expressed.

4. Conclusions

In this paper, an observation on the toe pads of a newt was carried out and the micro- and nano-structure of polygonal columnar epithelial cells separated by networking channels were found on their toe pads. It is believed that the stability of newt's crawling motion is closely related to its toe pads' structure.

Inspired by the surface structure, elastic micro-dimple and -pillar patterned surfaces were fabricated in PDMS to explore the effect of surface micro-structure on its tribological performance. The friction behaviours of the patterned surfaces lubricated with deionized water were evaluated. The experimental results shows that the PDMS surface with micro-dimples displayed a reduction in friction with an increase in the pattern area density. The area density of pillar patterns had no significant effect on the friction property at low sliding speeds, whereas it became a dominating factor with the increase of sliding speed. The friction force versus area density relationship is approximately linear increase for a pillar patterned surface and is likely one of the reasons that the polygonal columnar structure of newts' toe pads evolved.

Acknowledgments

This research was supported by the National Nature Science Foundation of China (NSFC) (Nos. U1134003 and 51175246) and Priority Academic Program Development of Jiangsu Higher Education Institutions (PAPD).

References

[1] Barthlott W and Neinhuis C 1997 Purity of the sacred lotus, or escape from contamination in biological surface *Planta* **202** 1–8
[2] Gao X and Jiang L 2004 Water-repellent legs of water striders *Nature* **432** 36
[3] Autumn K, Liang Y A, Hsieh S T, Zesch W, Chan W P, Kenny T W, Fearing R and Full R J 2000 Adhesive force of a single gecko foot-hair *Nature* **405** 681–4
[4] Naik V M, Mukherjee R, Majumder A and Sharnma A 2009 Super functional materials: creation and control of wettability, adhesion and optical effects by meso-texturing of surfaces *Current Trends in Science: Platinum Jubilee Special* (Bangalore: Indian Academy of Sciences) pp 129–48
[5] Yu H, Huang W and Wang X 2013 Dimple patterns design for different circumstances *Lubr. Sci.* **25** 67–78
[6] Federle W, Barnes W J P, Baumgartner W, Dreschler P and Smith J M 2006 Wet but not slippery: boundary friction in tree frog adhesive toe pads *J. R. Soc. Interface* **3** 689–97
[7] Barnes W J P, Goodwyn P J P, Nokhbatolfoghahai M and Gorb S N 2011 Elastic modulus of tree frog adhesive toe pads *J. Comp. Physiol.* A **197** 969–78
[8] Drotlef D-M, Stepien L, Kappl M, Barnes W J P, Butt H-J and del Campo A 2013 Insights into the adhesive mechanisms of tree frogs using artificial mimics *Adv. Funct. Mater.* **23** 1137–46
[9] Xiao L J, Wang X J and Li Q 2010 Bionic design of the surface morphology of rubber bush covered on driving drums *Adv. Nat. Sci.* **3** 120–7
[10] Gorb S, Jiao Y and Scherge M 2000 Ultrastructural architecture and mechanical properties of attachment pads in Tettigonia viridissima (Orthoptera Tettigoniidae) *J. Comp. Physiol.* A **186** 821–31
[11] Persson B N J 2007 Wet adhesion with application to tree frog adhesive toe pads and tires *J. Phys.: Condens. Matter* **19** 376110
[12] Scholz I, Barnes W J P, Smith J M and Baumgartner W 2008 Ultrastructure and physical properties of an adhesive surface, the toe pad epithelium of the tree frog, Litoria caerulea White *J. Exp. Biol.* **212** 155–62
[13] Hanna G and Barnes W J P 1991 Adhesion and detachment of the toe pads of tree frogs *J. Exp. Biol.* **155** 103–25
[14] Barnes W J P 2007 Functional morphology and design constraints of smooth adhesive pads *MRS Bull.* **32** 479–85
[15] Varenberg M and Gorb S N 2009 Hexagonal surface micropattern for dry and wet friction *Adv. Mater.* **21** 483–6
[16] Poulard C, Restagno F, Weil R and Légera L 2011 Mechanical tunning of adhesion through micro-patterning of elastic surfaces *Soft Matter* **7** 2543–51
[17] Huang W, Jiang L, Zhou C and Wang X 2012 The lubricant retaining effect of micro-dimples on the sliding surface of PDMS *Tribol. Int.* **52** 87–93
[18] He B, Chen W and Jane W Q 2008 Surface texture effect on friction of a microtextured poly(dimethylsiloxane) (PDMS) *Tribol. Lett.* **31** 187–97
[19] Martin A, Clain J, Buguin A and Brochard-Wyart F 2002 Wetting transitions at soft, sliding interfaces *Phys. Rev.* E **65** 031605
[20] Degrandi-Contraires E, Poulard C, Restagno F and Léger L 2012 Sliding friction at soft micropatterned elastomer interfaces *Faraday Discuss.* **156** 255–65
[21] Zhang B, Huang W and Wang X 2012 Biomimetic surface design for ultrahigh molecular weight polyethylene to improve the tribological properties *Proc. Inst. Mech. Eng. J* **226** 705–13